Numerical Simulation of the Propagation of Plasma Waves near the Earth's Magnetopause

Johan De Keyser

Belgian Institute for Space Aeronomy
Ringlaan 3, B-1180 Brussels
Johan.DeKeyser@bira-iasb.oma.be

The magnetopause: a natural lab for wave propagation

The Sun produces a continuous outward stream of ionized particles, a magnetized plasma called the solar wind that is variable on time scales from seconds to centuries. Major explosions ("mass ejections") on the Sun produce "stormy conditions in the solar wind.

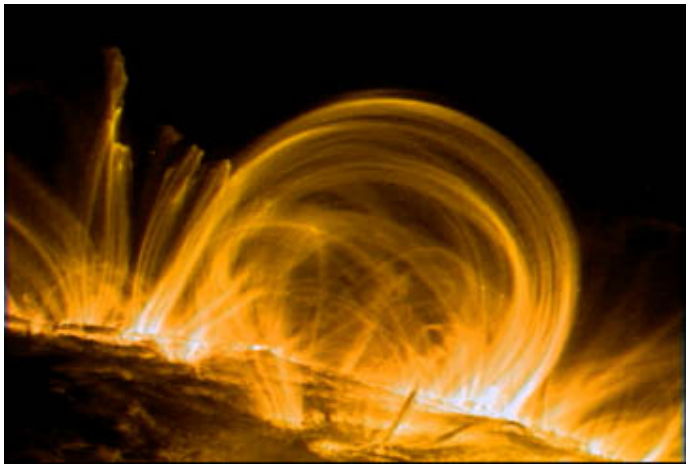

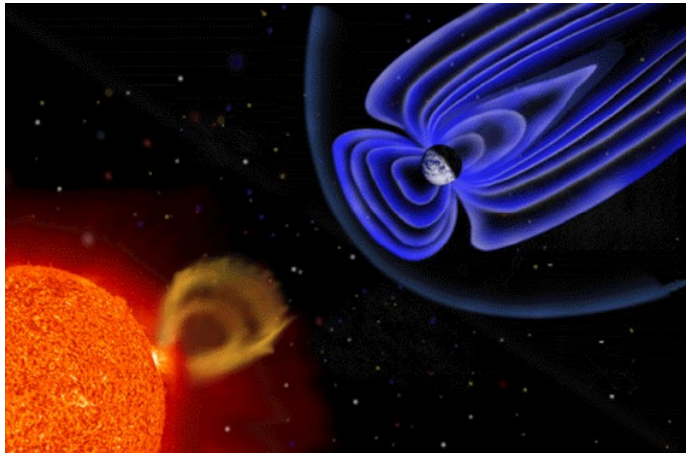

The Earth and its surrounding magnetic field form an obstacle for the solar wind, forming a bow shock (where the solar wind becomes subsonic) and the magnetopause. The region between bow shock and magnetopause is the magnetosheath.

Solar wind variations or plasma waves “shake” the magnetosphere and influence mass and energy transport into the magnetosphere.

Space weather affects the radiation level in robotic and manned spacecraft (communication satellites, ISS, ...), auroral lights, induced currents in power grids, corrosion of oil pipelines, disturbed radio signals, radiation dose received by high-altitude airplanes flying in the auroral regions.



Modeling plasma dynamics

Plasma dynamics is a conservation problem in 6+1 dimensions. The unknowns are the phase space densities for all plasma species, which depend on the 3 space dimensions, 3 velocity components, and time.

Major simplification: Assume that the velocity distributions are Maxwellian and use the moments of the velocity distributions. The problem is then similar to hydrodynamics, in 3+1 dimensions, with electric and magnetic forces are added. The unknowns are the densities, temperatures, and mean velocities of the species involved.

Further simplification: Forget about charge separation and electric fields, except for the electric field from the Lorentz transform. Consider only one ion species.

We make assume that the plasma is cold.

Cold magnetohydrodynamics equations

$$\frac{\partial \rho}{\partial t} + \nabla \cdot (\rho \mathbf{v}) = 0, \tag{1}$$

$$\frac{\partial \rho \mathbf{v}}{\partial t} + \nabla \cdot [\rho \mathbf{v}\mathbf{v} + \frac{B^2}{2\mu_0}\mathbf{I} - \frac{1}{\mu_0}\mathbf{B}\mathbf{B}] = \mathbf{0}, \tag{2}$$

$$\mathbf{E} + \mathbf{v} \times \mathbf{B} = \eta \mu_0 \mathbf{j}, \tag{3}$$

$$\nabla \times \mathbf{B} = \mu_0 \mathbf{j}, \tag{4}$$

$$\frac{\partial \mathbf{B}}{\partial t} + \nabla \times \mathbf{E} = \mathbf{0}, \tag{5}$$

$$\nabla \cdot \mathbf{B} = 0. \tag{6}$$

Linearized equations

Model the plasma at the magnetopause by a 1-D equilibrium + small-amplitude waves
$\mathbf{q}(x,y,z,t) = \mathbf{q}^{(0)}(x) + \mathbf{q}^{(1)}(x,y,z,t)$

State vector $\mathbf{q}^{(1)} = [v_x^{(1)}, v_y^{(1)}, B_x^{(1)}, B_y^{(1)}, B_z^{(1)}]$ ($v_z^{(1)} \equiv 0$)

Linearized cold MHD or wave propagation equations (hyperbolic system)

$$\frac{\partial \mathbf{q}^{(1)}}{\partial t} + v_A(\mathcal{A}_x\frac{\partial}{\partial x} + \mathcal{A}_y\frac{\partial}{\partial y} + \mathcal{A}_z\frac{\partial}{\partial z})\mathbf{q}^{(1)} = \eta\mathcal{C}\nabla^2\mathbf{q}^{(1)}, \tag{7}$$

$$\mathcal{A}_x = \begin{bmatrix} . & . & . & . & b^{-2} \\ . & . & . & . & . \\ . & . & . & . & . \\ . & . & . & . & . \\ b^2 & . & . & . & . \end{bmatrix}, \mathcal{A}_y = \begin{bmatrix} . & . & . & . & . \\ . & . & . & . & b^{-2} \\ . & . & . & . & . \\ . & . & . & . & . \\ . & b^2 & . & . & . \end{bmatrix}, \mathcal{A}_z = \begin{bmatrix} . & . & -b^{-2} & . & . \\ . & . & . & -b^{-2} & . \\ -b^2 & . & . & . & . \\ . & -b^2 & . & . & . \\ . & . & . & . & . \end{bmatrix}, \mathcal{C} = \begin{bmatrix} . & . & . & . & . \\ . & . & . & . & . \\ . & . & 1 & . & . \\ . & . & . & 1 & . \\ . & . & . & . & 1 \end{bmatrix},$$

where $b^2 = B^{(0)}/v_A$

Physical interpretation

Waves in uniform medium :

$\mathbf{q}^{(1)} \propto \exp i(k_x x + k_y y + k_z z - \omega t)$

Dispersion relation $(\omega^2 - k_z^2 v_A^2)(\omega^2 - k^2 v_A^2) = 0$

Alfvén mode and fast-mode waves: not isotropic because of $\mathbf{B}$

Nonuniformity along x :

$\mathbf{q}^{(1)} \propto \hat{\mathbf{q}}(x) \exp i(k_y y + k_z z - \omega t)$

Even if BCs $\equiv 0$ there are nontrivial solutions with $\omega^2 - k_z^2 v_A^2 = 0$

Alfvén waves propagating parallel to the y,z-plane: surface waves

If $\eta > 0$: diffusion provides resonant mode coupling where $v_A(x^*) = \pm\omega/k_z$

Numerical solution

Set $q^{(1)}(x,y,z,t) = \hat{\mathbf{q}}(x,t)\exp i(k_y y + k_z z)$, then $\frac{\partial}{\partial y} \rightarrow ik_y$, $\frac{\partial}{\partial z} \rightarrow ik_z$

Special scaling $\tilde{\mathbf{q}} = [b\hat{v}_x, ib\hat{v}_y, i\hat{B}_x/b, \hat{B}_y/b, \hat{B}_z/b]$: constant and real flux jacobians

$$\frac{1}{v_A}\frac{\partial \tilde{\mathbf{q}}}{\partial t} + \tilde{\mathcal{A}}_x \frac{\partial}{\partial x}\tilde{\mathbf{q}} = -(k_y\tilde{\mathcal{A}}_y + k_z\tilde{\mathcal{A}}_z + \frac{1}{b}\frac{db}{dx}\tilde{\mathcal{S}})\tilde{\mathbf{q}} + \frac{\eta}{v_A}[(\frac{1}{b}\frac{d^2b}{dx^2} - k_y^2 - k_z^2) + \frac{2}{b}\frac{db}{dx}\frac{\partial}{\partial x} + \frac{\partial^2}{\partial x^2}]\tilde{\mathcal{C}}\tilde{\mathbf{q}}, \qquad (8)$$

with

$$\tilde{\mathcal{A}}_x = \begin{bmatrix} . & . & . & . & 1 \\ . & . & . & . & . \\ . & . & . & . & . \\ . & . & . & . & . \\ 1 & . & . & . & . \end{bmatrix}, \tilde{\mathcal{A}}_y = \begin{bmatrix} . & . & . & . & . \\ . & . & . & . & -1 \\ . & . & . & . & . \\ . & . & . & . & . \\ . & 1 & . & . & . \end{bmatrix}, \tilde{\mathcal{A}}_z = \begin{bmatrix} . & . & -1. & . & . \\ . & . & . & 1 & . \\ 1 & . & . & . & . \\ . & -1. & . & . & . \\ . & . & . & . & . \end{bmatrix}, \tilde{\mathcal{S}} = \begin{bmatrix} . & . & . & . & 1 \\ . & . & . & . & . \\ . & . & . & . & . \\ . & . & . & . & . \\ -1. & . & . & . & . \end{bmatrix}, \tilde{\mathcal{C}} = \mathcal{C}$$

Spatial Discretization

Finite-volume discretization with equidistant mesh Ω_i with spacing h

$$\frac{1}{v_{A,i}}\frac{\partial \tilde{\mathbf{q}}_i}{\partial t}+\frac{1}{h}[\tilde{\mathbf{f}}_{x,i+\frac{1}{2}}-\tilde{\mathbf{f}}_{x,i-\frac{1}{2}}]=\tilde{\mathbf{g}}_i,$$

with $\tilde{\mathbf{q}}_i=\int_{\Omega_i}\tilde{\mathbf{q}}(x,y,z)\mathrm{d}\Omega/h$ and similarly cell-averaged rhs $\tilde{\mathbf{g}}_i$

Numerical flux: Roe-type approximate Riemann solver

$$\tilde{\mathbf{f}}_{x,i+\frac{1}{2}}=\frac{1}{2}[\tilde{\mathbf{f}}_x(\tilde{\mathbf{q}}_L)+\tilde{\mathbf{f}}_x(\tilde{\mathbf{q}}_R)-\tilde{\mathbf{d}}_x(\tilde{\mathbf{q}}_L,\tilde{\mathbf{q}}_R)]$$

with $\tilde{\mathbf{f}}_x(\tilde{\mathbf{q}})=\tilde{\mathcal{A}}_x\tilde{\mathbf{q}}$ and $\tilde{\mathbf{d}}_x=\Sigma_\alpha\,|\tilde{\lambda}_x^\alpha|\tilde{\mathbf{r}}_x^\alpha\tilde{\mathbf{l}}_x^\alpha(\tilde{\mathbf{q}}_R-\tilde{\mathbf{q}}_L)=\begin{bmatrix}\tilde{v}_{xR}-\tilde{v}_{xL}\\ \cdot\\ \cdot\\ \cdot\\ \tilde{B}_{zR}-\tilde{B}_{zL}\end{bmatrix}$,

where $\tilde{\lambda}_x^\alpha$, $\tilde{\mathbf{r}}_x^\alpha$, and $\tilde{\mathbf{l}}_x^\alpha$ are eigenvalues and right and left eigenvectors of constant $\tilde{\mathcal{A}}_x$

Spatial accuracy order depends on interpolation used for $\tilde{\mathbf{q}}_L$ and $\tilde{\mathbf{q}}_R$

It must be (at least) second-order to capture dissipative term:

$$\tilde{q}_L = \tilde{q}_i + \frac{h}{2}\phi(\frac{\nabla_+\tilde{q}_{i+1}}{\nabla_-\tilde{q}_i})\nabla_-\tilde{q}_i, \tag{9}$$

$$\tilde{q}_R = \tilde{q}_{i+1} - \frac{h}{2}\phi(\frac{\nabla_-\tilde{q}_i}{\nabla_+\tilde{q}_{i+1}})\nabla_+\tilde{q}_{i+1}, \tag{10}$$

where $\nabla_+\tilde{q}_{i+1} = (\tilde{q}_{i+2} - \tilde{q}_{i+1})/h$ and $\nabla_-\tilde{q}_{i+1} = (\tilde{q}_{i+1} - \tilde{q}_i)/h$.

Flux limiter ϕ adds diffusion near discontinuities in the solution so that the spatial accuracy is of order one there, while it remains effectively second-order elsewhere.

Time Discretization

System (8) is first-order in time.

Explicit time integration with Courant-Friedrichs-Lewy limit $\Delta t_{\mathrm{CFL}} = h/v_A$

Define residual at timestep l

$$\tilde{\mathcal{R}}\tilde{\mathbf{q}}_{l,i} = v_{A,i}[\tilde{\mathbf{g}}_{i,l} - \frac{1}{h}(\tilde{\mathbf{f}}_{x,i+\frac{1}{2},l} - \tilde{\mathbf{f}}_{x,i-\frac{1}{2},l})].$$

Forward Euler is first-order accurate in time

$$\tilde{\mathbf{q}}_{l+1} = \tilde{\mathbf{q}}_l + \Delta t_l \tilde{\mathcal{R}}\tilde{\mathbf{q}}_l.$$

Multi-stage Runge-Kutta: RK2($\frac{1}{2}$,1) is second-order accurate in time

$$\begin{aligned} \tilde{\mathbf{q}}_{l+\frac{1}{2}} &= \tilde{\mathbf{q}}_l + \frac{1}{2}\Delta t_l \tilde{\mathcal{R}}\tilde{\mathbf{q}}_l, \\ \tilde{\mathbf{q}}_{l+1} &= \tilde{\mathbf{q}}_l + \Delta t_l \tilde{\mathcal{R}}\tilde{\mathbf{q}}_{l+\frac{1}{2}}. \end{aligned}$$

Magnetopause equilibrium

Consider a planar magnetopause of finite thickness parallel to yz.

The magnetosphere is largely void compared to magnetosheath.

The Alfvén speed changes by an order of magnitude: resonance can occur.

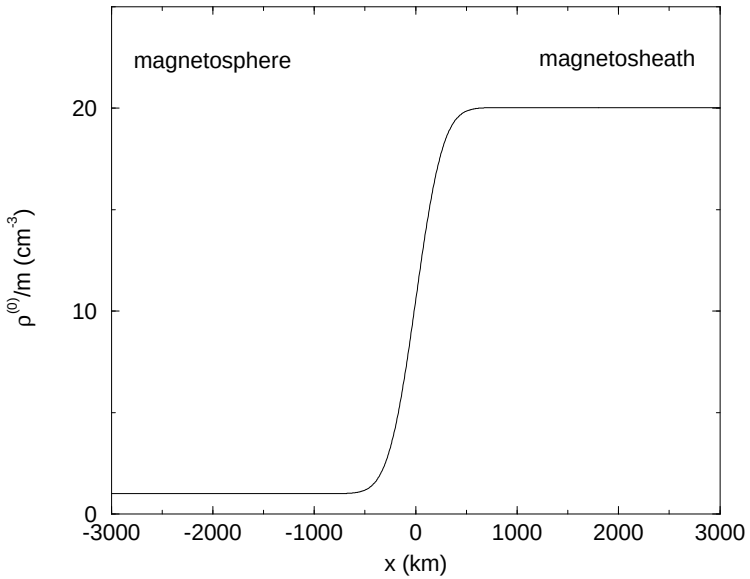

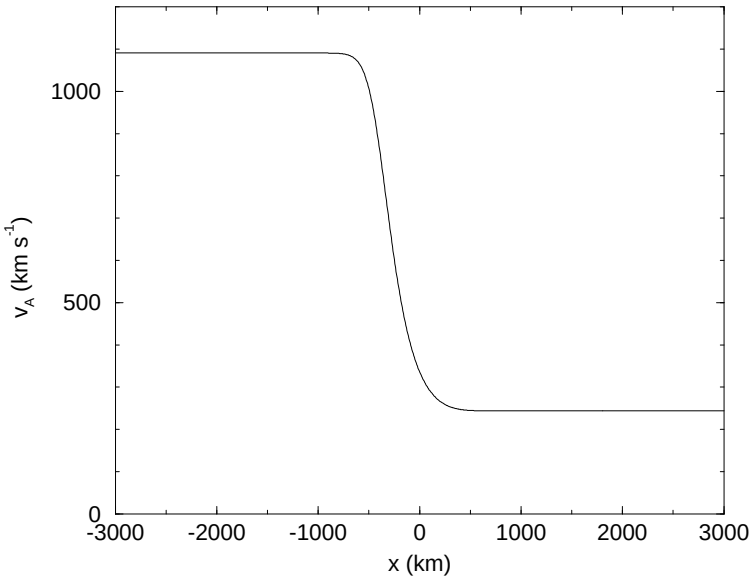

Initial Condition and Boundary Conditions

Initial condition

- unperturbed system $\hat{\mathbf{q}}(x, t_0 = 0) \equiv \mathbf{0}$

Boundary conditions

- no wave enters the domain on the magnetospheric side
- incident monochromatic fast-mode wave on the magnetosheath side starts at $t_0 = 0$
- for specified frequency, $\mathbf{k}$ must satisfy the magnetosheath dispersion relation
- the boundary conditions define the arbitrary scaling of $\mathbf{q}$
- discontinuities at $t_0 = 0$ may require flux limiter
- the Riemann solver ensures that outgoing waves simply leave the domain

Transient Development of a Resonant Sheet

- frequency $f = 0.5$ Hz, incidence $\phi = 135°$, $\theta = 45°$, diffusivity $\eta = 5 \times 10^6$ m^2 s^{-1}
- RK2, $\tau_{\mathrm{CFL}} = 0.5$, second-order in space, minmod limiter, 2000 points, 40 periods

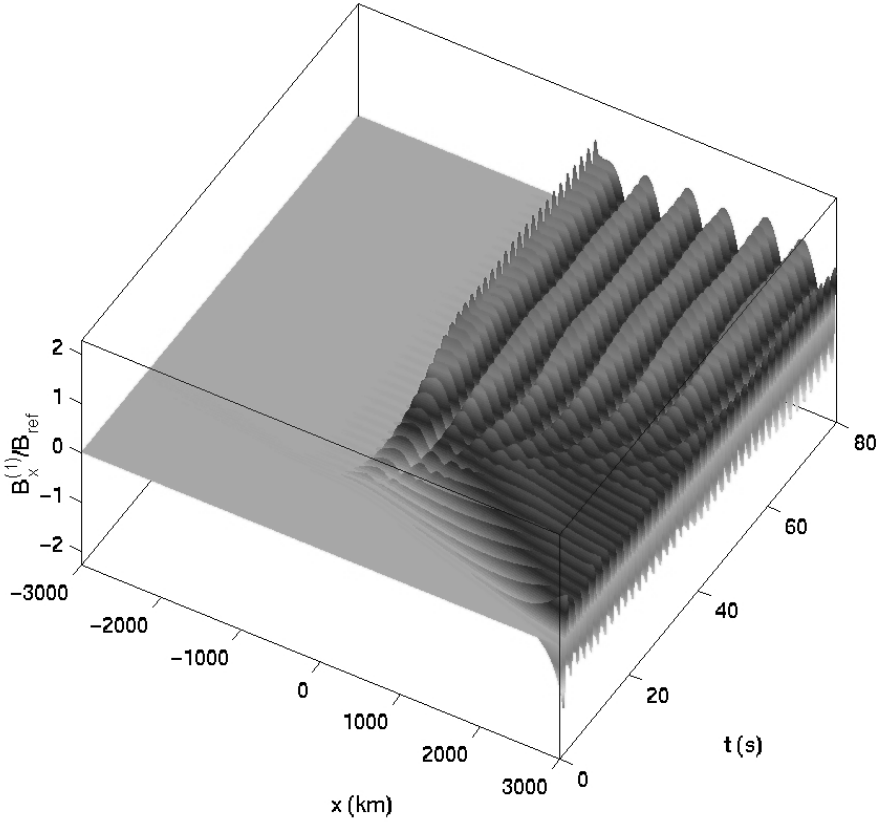

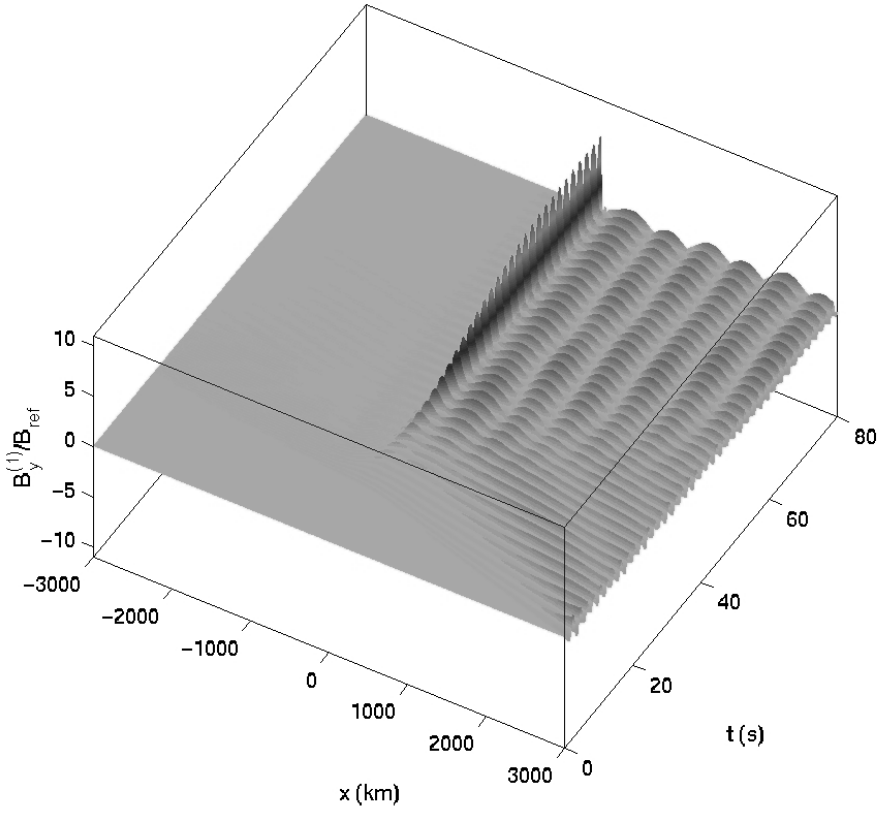

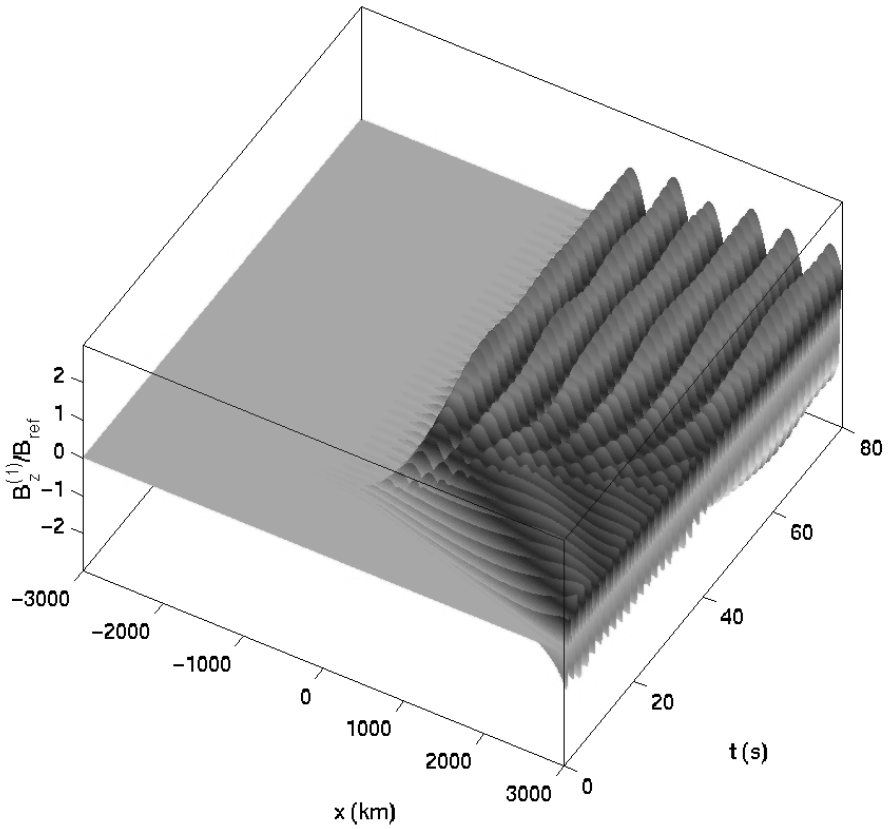

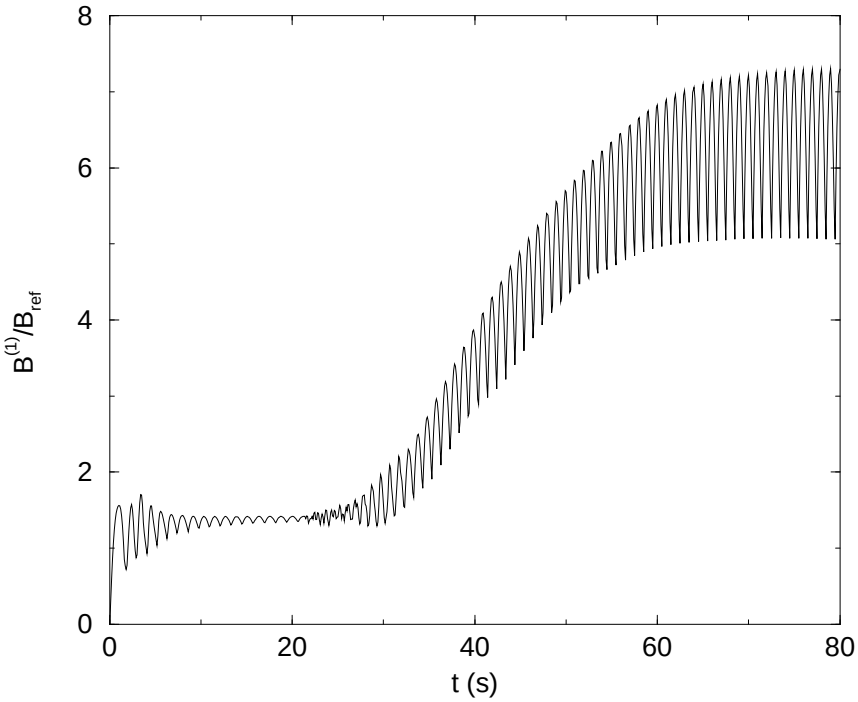

- partial absorption and reflection, no transmission in this case
- initial exponential growth of resonant amplitude, which saturates due to diffusion

Spatial resolution

For $\eta = 0$ the resonant waves are fully decoupled and the layer is infinitely thin.
But discretization introduces numerical diffusion, resulting in a finite-amplitude resonant peak with nonzero width that depends on the method and the mesh.

We always use physical diffusion $\eta > 0$ that exceeds the numerical diffusion so as to obtain mesh-independent results:

- The resonant layer is only 50 km thick in the example (thinner as η decreases)
- ... or 16 mesh points, so that it is well-resolved.
- Verified by doubling the number of mesh points.

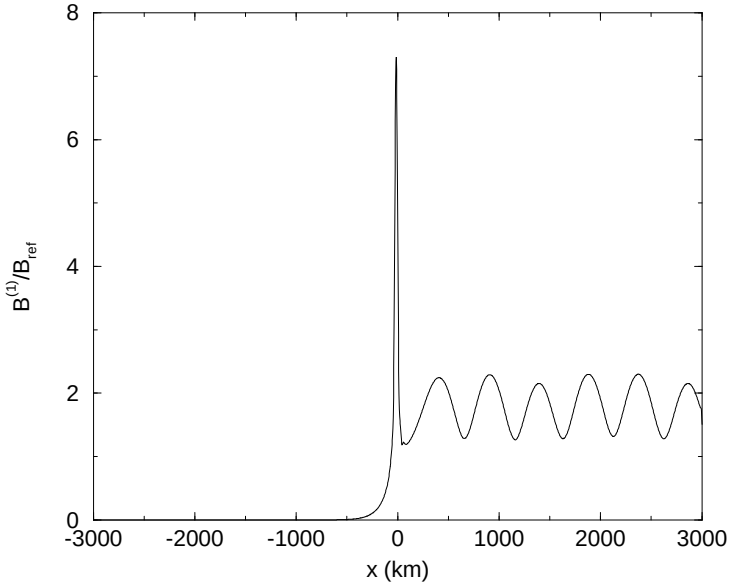

Analogy with hydrodynamics: Euler and Navier-Stokes equations

Relation between spatial and temporal discretization

Mesh spacing h must resolve the wavelength: $hk \ll 1$

Stability condition: $\tau_{\mathrm{CFL}} = \Delta t / \Delta t_{\mathrm{CFL}}$ is of order 1.

Then $\omega \Delta t = \omega \tau_{\mathrm{CFL}} \Delta t_{\mathrm{CFL}} = \tau_{\mathrm{CFL}} h\omega / v_A = \tau_{\mathrm{CFL}} hk \ll 1$:
the time scale imposed by the boundary conditions is resolved too

Limited use for implicit methods: time step cannot be much larger for accuracy reasons

... unless resonant layer thickness is much smaller than the wavelength

Total discretization error

Relative FE total discretization error $\epsilon_l \sim l\frac{\tau_{\text{CFL}}^2}{2}(hk)^2$

Solution is worthless when $\epsilon_l \sim 1$ or $l_{\max} \sim \frac{2}{\tau_{\text{CFL}}^2(hk)^2}$

Maximum time: $t_{\text{sim}} = l_{\max}\Delta t \sim \frac{2}{\tau_{\text{CFL}}(hk)(kv_A)} = \frac{T}{\tau_{\text{CFL}}\pi hk}$ or $\nu \sim (hk)^{-1}$ periods

Relative RK2 total discretization error $\epsilon_l \sim l(hk)^3$

Maximum number of timesteps: $l_{\max} \sim \frac{1}{(hk)^3}$

Maximum time $t_{\text{sim}} = l_{\max}\Delta t \sim \frac{\tau_{\text{CFL}}}{2\pi}\frac{T}{(hk)^2}$, or $\nu \propto (hk)^{-2}$ periods

Summary

- Forward Euler: $l_{\max} \propto (hk)^{-2}$ timesteps, each at $\sim (hk)^{-1}$ points
  as $\nu \propto (hk)^{-1}$ the computational complexity is $(hk)^{-3} \propto \nu^3$.
- RK2: $l_{\max} \propto (hk)^{-3}$, each requires two updates at $\sim (hk)^{-1}$ mesh points
  as $\nu \propto (hk)^{-2}$ the computational complexity is $(hk)^{-4} \propto \nu^2$

Energy Balance

Net (time-averaged) energy flux is a second-order quantity.

In a cold plasma: Poynting flux $\langle P_x^{(2)} \rangle = \frac{1}{\mu_0} \langle \mathbf{E}^{(2)} \times \mathbf{B}^{(0)} + \mathbf{E}^{(1)} \times \mathbf{B}^{(1)} \rangle_x = \frac{1}{\mu_0} \frac{\cos\phi}{\cos\theta} v_A B_{z,\mathrm{peak}}^{(1)2}$.

A physical and numerical check on the conservation of energy.

Normal incidence case: no resonant absorption, but partial transmission and reflection

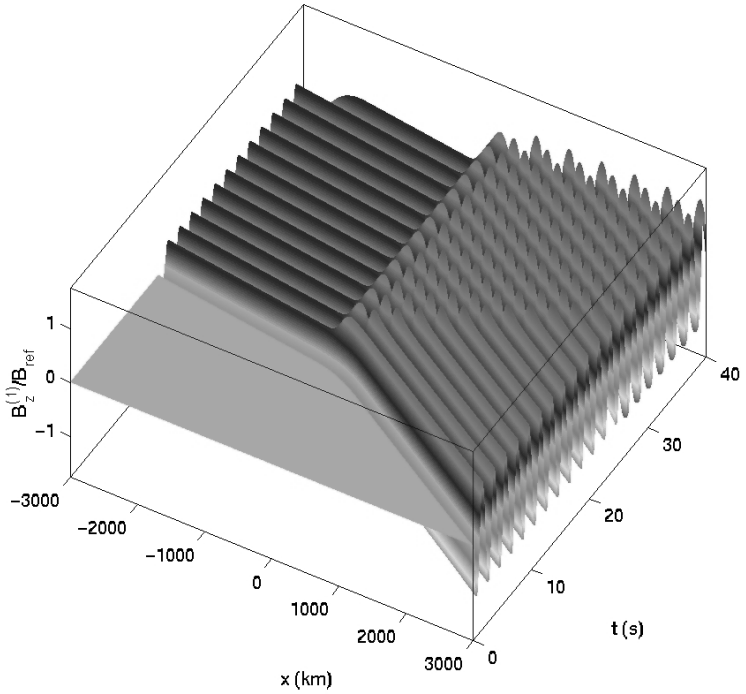

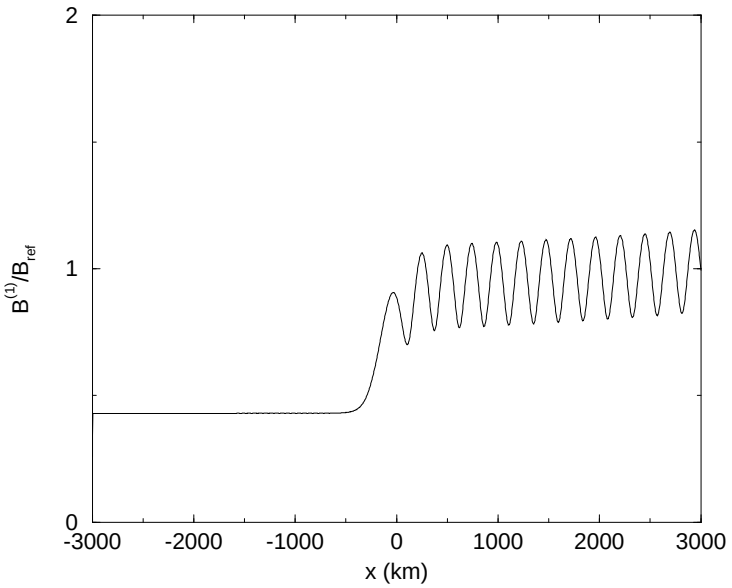

Conclusions

Codes should take advantage of the close relationship between physics and numerics.

Both high spatial and temporal accuracy are needed to be able to conduct the simulation precisely enough (resolving the resonant sheet) and long enough (until saturation).

Computational complexity increases fast when the dissipation becomes smaller.

There are no monochromatic wave that last long enough to drive sharp peaks in thin layers, but rather broadband waves that enhance the fluctuation amplitudes throughout the magnetopause layer.

Reality is nonlinear.

The true geometry and coupling with the ionosphere should be taken into account.

Magnetohydrodynamics is not completely justified at the magnetopause ...

Acknowledgements

This work was supported by PRODEX in the context of
ESA's Ulysses and Cluster II missions.
Thanks also goes to the Belgian Federal Office for
Scientific, Technical and Cultural Affairs.